

# V-f Control of Solar Photovoltaic Output Power Isolated From Grid

Jajula Kiran<sup>1</sup>, M.Ravi Kumar<sup>2</sup>

<sup>1</sup>(M.Tech Student EEE Department, Prasad V.Potluri Siddhartha Institute of Technology, A.P,India)

<sup>2</sup>(Assistant Professor, EEE Department, Prasad V.Potluri Siddhartha Institute of Technology, A.P, India)

## ABSTRACT:

The wished-for Coordinated V-f Control of Solar Photovoltaic output power with MPPT and Battery Storage in Microgrids to act in a coordinated way to provide vital control over the voltage and frequency by controlling the necessary quantity of active power and auxiliary service once needed. The microgrid is medium voltage level utility grid via circuit breaker when it hooked up to the grid, consequently, it is operated as load bus (PQ). Due to the fact that grid controls voltage and frequency of microgrid and once it is remoted from grid it operates as generator bus (PV). At that situation, there is a risk taking place in voltage and frequency deviation. So several control methods have the capability of controlling V-f in both grid and microgrid is harnessed. By using control methods like MPPT control at PV side battery and V-f at the PV and inverter side. The major novelty of system lies within the coordination among individual with proportional and integral (PI) controller. An effective coordination among participating micro resources while considering the case of dynamical irradiance and battery state of charge (SOC) constraint. A coupling inductor and capacitor placed in between PV system and grid, for the elimination of ripples and injects reactive power to PV system. Also, battery storage supports the PV system while in emergencies. This arrangement helps to keep the microgrid voltage and frequency constant and reliable supply to the critical loads.

*Index Terms:* microgrid, standalone, hourly solar irradiance, voltage and frequency control, distributed generation (DG), battery state of charge (SOC).

## INTRODUCTION

An ever increasing demand for energy and environmental concerns in the 21<sup>st</sup> century has led to a sustained effort to generate power from various alternative energy resources. Although coal and hydropower plants are still used to produce electric power on a large scale, renewable energy has been of primary focus in recent years due to their abundance. With issues such as global warming and depletion of fossil fuels, generation from alternative energy resources such as the wind and solar power has been increasing steadily. The rate at which photovoltaic (PV) power generation is projected to increase by 2030 is promising in many aspects.

The microgrid could be an assortment of distributed generators micro resources, energy storage devices, and loads that operate as a single and independently manageable system capable of providing each power and heat to the area of service [2]. The microresources that are incorporated in a microgrid are comprised of tiny units, less than 100 kilowatts, A microgrid is typically built around medium voltage level distribution systems with distributed energy resources (DERs) such as micro-turbines, fuelcells, PV arrays, etc. provided with the electronics (PE) interface. In a microgrid, the micro sources and storage devices are associated to the feeders through the micro source controllers (MCs) and the coordination among the micro sources is carried out by the central controller (CC) [3]. The microgrid is medium voltage level utility grid via circuit breaker when it hooked up to the grid consequently, it is operated as load bus (PQ).

Due to the fact that grid controls voltage and frequency of microgrid and once it is remoted from grid it operates as generator bus (PV). The operation and management in both the modes is controlled and coordinated with the facilitate of microsource controllers (MCs) at the native level and central controller (CCs) at the global level Similar to the standard synchronous generator frequency control [4], the microgrid voltage and frequency management will additionally be performed using droop control strategies [5]–[9]. The present

work provides quick response characteristics for voltage and frequency management as compared to the secondary management considered in [8]. The associate log between inverter control and the synchronous generator control in an islanded microgrid is studied thoroughly in [9]. In the islanded mode, there is the requirement of getting a standard voltage and frequency signals within the microgrid inverter control [10]. The operation and control of the inverter interface of renewable- primarily based distributed energy resources (DERs), like Solar photovoltaic (PV) in a microgrid, is a real challenge, especially once it comes to maintaining each microgrid voltage and frequency within an appropriate range. A voltage management methodology primarily based on ancient droop control for voltage sag mitigation in conjunction with voltage ride through capability is proposed in [11]. A dynamic voltage regulation based on adaptive control is planned in [12], [13]. However, there are not several analysis works performed on V-f management using solar PV as well as MPPT control and battery storage in microgrids. In [14], frequency regulation with PV in microgrids is studied; however, this work does not take into account the voltage management objective and lacks battery storage within the microgrid. In [15], a small-scale PV is taken into account during a grid-connected mode to regulate the active and reactive power of the system. Here, the control strategies take into account abc-dq0 transformation and vice versa that is avoided in the present paper. In [16], power modulation of solar PV generators with associated electrical double layer capacitance as energy storage is taken into account for frequency control. In [17], load frequency control is enforced in amicrogrid with PV and storage; but, this work also lacks the consideration of a voltage control objective.

The voltage associated frequency control with solar PV and battery in amicrogrid with an induction machine is investigated in [18]; but, this work does not justify the transfer mechanism of controls to contemplate the dynamical irradiance and battery state of charge (SOC) constraint. In summary, the previous works on this topic either lack the incorporation of an energy storage element or the voltage control objective in conjunction with frequency management or the incorporation of control transition in several situations. The present work fulfills these gaps by considering all of those objectives

## SYSTEM CONFIGURATION

Fig. 1 shows the PV system configuration for V-F control whereas PV operative at MPP together with the battery storage backup. It is a two-stage configuration where a DC-DC boost device is used for MPPT control. The system also considers a battery back-up just in case of emergencies while maintaining the voltage of the microgrid or while trying to provide the crucial loads. A battery is connected in parallel to the PV to inject or absorb active power through a bidirectional DC-DC converter. When the battery fascinating power, the converter operates in the buck mode and once thebattery is injecting power to the grid, it operates in the boost mode. The operation mode is maintained through the control signal provided to the converter switches. The PV system is connected to the grid through a coupling inductor. The coupling inductor filters out the ripples in the PV output current. The connection point is called the point of common coupling (PCC) and therefore the PCC voltage is denoted as  $V_{(t)}$ .

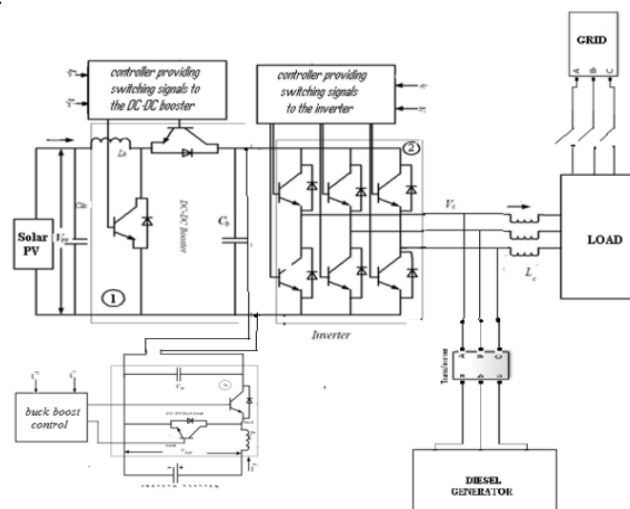


**Fig. 1:** System configuration of V-f control with solar PV generator operating at MPPT With a battery storage system

The PV source is connected to the DC link of the inverter with a capacitor. The PV is the active power source, and the capacitor is that the reactive power source of the PV system. The anticipated control strategy additionally provides a switch transition of PV side PQ management in grid connected mode to V-f control in islanded mode. These control algorithms are additionally capable of handling the battery SOC constraint. The anticipated V-f control methodology shows a very satisfactory performance in bringing back the extremely reduced voltage and frequency back to the nominal values in short time.

According to the instantaneous power definitions, for a balanced three-phase system, if  $V_t(t)$  and  $V_c(t)$  denote the instantaneous PCC voltage and the inverter output voltage (harmonics neglected), respectively, then the average power of the PV denoted as  $P(t)$ , the apparent power  $S(t)$  and the average reactive power  $Q(t)$  of the PV are as given below [20].

$$p(t) = \frac{2}{T} \int_{t-\frac{T}{2}}^t v_i(t) i_c(t) dt = \frac{V_t(t) V_c(t)}{\omega L_c} \sin \alpha \quad (1)$$

$$P(t) \approx \frac{V_t(t) V_c(t)}{\omega L_c} \alpha \quad (1a)$$

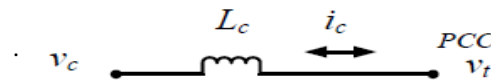


**Fig. 2:** Simplified circuit diagram of a parallel-connected PV

Let  $v_t(t)$  and  $V_c(t)$  denote the instantaneous PCC voltage and the inverter output voltage (harmonics are neglected) respectively, where  $\alpha$  is the phase angle of  $V_c(t)$  relative to the PCC Voltage.

$$V_t(t) = \sqrt{\frac{2}{T} \int_{t-\frac{T}{2}}^t v_t^2(\tau) d\tau} \quad (2)$$

$$V_c(t) = \sqrt{\frac{2}{T} \int_{t-\frac{T}{2}}^t v_c^2(\tau) d\tau} \quad (3)$$

$$S(t) = V_t(t) I_c(t) = \sqrt{V_t(t)^2 + V_c(t)^2 - 2V_t(t)V_c(t) \cos \alpha} \quad (4)$$

The current from the inverter to the utility is denoted as  $i_c(t)$  given by equation (5).

$$i_c(t) = \frac{\sqrt{2}}{\omega L_c} [V_c \sin(\omega t + \alpha) - V_t \sin \omega t] \quad (5)$$

$$Q(t) = \sqrt{S^2(t) - P^2(t)} = \frac{V_t(t)}{\omega L_c} (V_c(t) \cos \alpha - V_t(t)) \quad (6)$$

$$Q(t) \approx \frac{V_t(t)}{\omega L_c} (V_t(t) - V_c(t)) \quad (6a)$$

Where,  $\alpha$  is the phase angle of  $V_c(t)$  relative to the PCC voltage.  $P(t)$  and  $Q(t)$  in (1) and (6) can be approximated by the first terms of the Taylor series if the angle  $\alpha$  is small, as shown in (1a) and (6a).

## MODELLING OF SOLAR PV

A detailed approach of PV cell modeling supported a mathematical description of the equivalent electrical circuit of a PV cell. Solar cells are the building blocks of a PV array. Basically solar cell is a P-N diode. The most commonly used configuration is the single-diode model. The circuit diagram of solar PV cell is

shown in below fig.3. The PV cell is capable of changing solar irradiance into dc current through the electrical phenomenon effect. [19].  $I_d$  is the ideal diode current which is in parallel with  $I_{ph}$ . Where  $R_{sh}$  &  $R_s$  are shunt and series resistances of solar cell respectively.

The current work uses the one-diode model of the photovoltaic cell to model the Kyocera KC200GT solar array. The reason to select this specific solar module is for simple validation of the simulated I-V curve with the experimentally accessible curve from the datasheet.

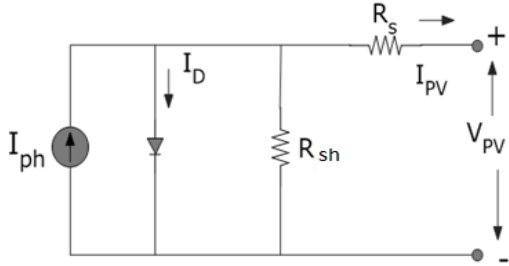


Fig. 3: single diode model of PV cell

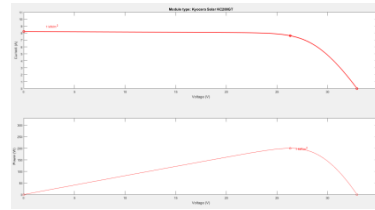


Fig. 4: V-I characteristics

The modeling is performed analytically based on the underlying equation of solar array V-I characteristics, as shown in Fig.4, are represented by the following mathematical equation (11).

The output current I of solar arrays [4] is given by equation (7) using Fig.3

$$I_{ph} = I_D + I_{Rp} + I \tag{7}$$

$$I = I_{ph} - I_d - V_d / R_{sh} \tag{8}$$

By applying the KVL in output loop of Fig.3, the resultant equation is

$$V_d = V + IR_s \tag{9}$$

$$I_D = I_0 \left( e^{V_D q / (nKT)} - 1 \right) \tag{10}$$

Substituting equations (9) & (10) in equation (8)

$$I = I_{pv} - I_0 \left( e^{\left( \frac{V + R_s I}{V_{therm} \alpha} \right)} - 1 \right) - \frac{V + R_s I}{R_{sh}} \tag{11}$$

$$I_{pv} = (I_{PV,n} + K_1 \Delta T) \frac{G}{G_n} \tag{12}$$

$$I_{PV,n} = \frac{R_{sh} + R_s}{R_{sh}} I_{sc} \tag{13}$$

Output of the solar PV cell depends on the irradiance. In this paper we have considered irradiance of particular location in India and parameters are given in Table 1. For 100 kW solar PV plant, during morning at 6AM irradiance is 0.05kW/m<sup>2</sup>, therefore, it generates 3.1KW of power. At 8AM it is shown as 0.399 kW/m<sup>2</sup> with 13.34kW of power as temperature increase irradiance increases as high as 0.844 kW/m<sup>2</sup> at 11AM it is 0.932kW/m<sup>2</sup> in the midafternoon which is the highest and the slowly decreases to 0.456kW/m<sup>2</sup> at 4PM and falls down to 0.125kW/m<sup>2</sup> at evening. Fig. 1 shows a graph of different irradiances values for each hour and the table shows PV output active power at different irradiances. So for experimental study, we are considering irradiance of 1.0 kW/m<sup>2</sup> so that maximum power can be generated from 100 kW solar PV plant.

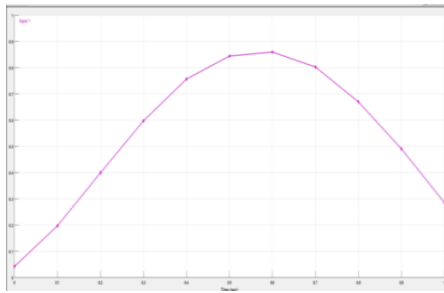


**Fig.4:** different irradiances values for each hour

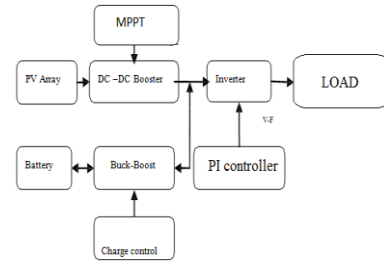


**Fig. 5:** ProposedSystemConfiguration

**Table 1:** Solar irradiance of the test feeder

Hour	Irradiance kW/m <sup>2</sup>	PV O/P from 100 kW plant
6	0.05	3.24
7	0.215	13.02
8	0.456	25.34
9	0.634	42.54
10	0.789	61.07
11	0.884	80.37
12	0.932	85.61
13	0.850	76.42
14	0.720	52.06
15	0.446	24.79
16	0.259	14.16
17	0.125	5.01

So to get 100kW solar power with  $I_{pv}$  and  $I_0$  are the photocurrent and the diode saturation currents respectively. The photocurrent of the PV array depends linearly on the solar irradiation and the cell temperature. PV Panel Parameters at 1000 W/m<sup>2</sup> and 25°C are shown in Table 2 The PV system under study for the projected V-f control has 125 strings with every string having 4 series connected panels. The Maximum power point (MPP) for one panel of KC200GT at 1000 W/m<sup>2</sup> and 25°C (STC) is 200 W. Hence, the maximum power of the PV generator at STC is 125 X 4 X 200 =100Kw [1]. But the MPP varies according to the modification in irradiance level and cell temperature.

**Table 2:**PV Panel Parameters at 1000 W/m<sup>2</sup> and 25°C

Model	Kyocera KC200GT
$P_{MPP}$	200W
$V_{MPP}$	26.30V
$I_{MPP}$	7.61A
$V_{OC}$	32.90V
$I_{sc}$	8.21A

### VOLTAGE AND FREQUENCY CONTROL METHODS

Proposed MPPT and Inverter side voltage controlled solar PV system is conferred in Fig.5. The control includes one loop for MPPT management and another loop for Voltage control at the inverter aspect. A typical solar panel converts solely 30 to 40 percent of the incident solar irradiation into electrical energy. Maximum power point technique is employed to improve the efficiency of the solar panel. According to Maximum Power

Transfer theorem, the power output of a circuit is maximum once the Thevenin resistivity of the circuit (Source impedance) matches with the load impedance. Hence our drawback of tracking the maximum power point reduced to impedance matching problem. In the sources side, we are using a boost device connected to a solar panel so as to boost the output voltage. By changing the duty cycle of the boost device we can set voltage to required value. In this paper MPPT at PV side is controlled using Incremental Conductance method. This Incremental Conductance method will confirm that the MPPT has reached the MPP and stop perturbing the in operation purpose. If this condition isn't met, the direction within which the MPPT operating point should be perturbed will be calculated using the connection between  $dI/dV$  and  $-I/V$ . This relationship taken from the actual fact that  $dP/dV$  is negative once the MPPT is to the right of the MPP therefore voltage is increased and if it is positive once it's to the left of the MPP therefore voltage is decreased. In according to this variation duty cycle is adjusted. This algorithm has benefits over P&O there in it will confirm once the MPPT has reached the MPP, wherever P&O oscillates round the MPP. Also, incremental conductance will track rapidly increasing and decreasing irradiance conditions with higher accuracy than P & O method. The disadvantage of the perturb and observe technique to track the peak power under quick varying climatic conditions is overcome by Incremental Conductance technique.

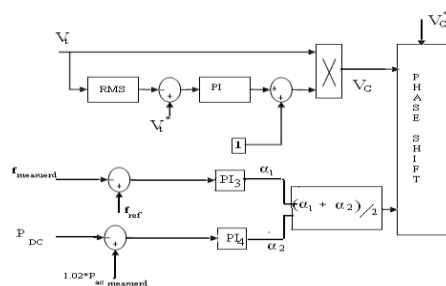


**Fig. 6:** Integrated Solar PV MPPT and V-f-control diagram

Proportional Integral (PI) controller  $PI_2$  is employed for voltage control at AC side of inverter, as shown in the control diagram in Fig.6. The rms value  $V_t(t)$  is compared with the voltage reference value  $V_t^*(t)$  and error is fed to  $PI_2$  controller, so that the PCC voltage is regulated at a given level. This controlling theme is specifically expressed as (16). Here  $K_{p2}$  and  $K_{I2}$  are control gains.

$$V_{c1}^* = V_t(t) \left[ 1 + K_{p2} (V_t^*(t) - V_t(t)) + K_{I2} \int_0^t (V_t^*(t) - V_t(t)) dt \right] \quad (16)$$

The frequency controlled by controlling the active power output at the inverter side therefore referenced microgrid frequency of 60 Hz is compared with the measured value and this error is fed to the  $PI_3$  controller that provides the phase shift contribution and the active power injected are enough to maintain the frequency at 60Hz nominal value. The equation for this control is given by (17)

$$\alpha_1^* = K_{p3} (f_{ref} - f_{measured}) + K_{I3} \int_0^t (f_{ref} - f_{measured}) dt \quad (17)$$

There is another controller employed in a similar. This controller maintains active power balance between the AC and DC sides of the inverter considering the efficiency of inverter as 98% such that the DC side active power is 102% of the AC side active power. The equation for this control is given by (18)

$$\alpha_2^* = K_{p4} (1.02 * P_{AC} - P_{DC}) + K_{I4} \int_0^t (1.02 * P_{AC} - P_{DC}) dt \quad (18)$$

The phase shift contributions from DC and AC sides, and are then averaged as given by (19)

$$\alpha^* = (\alpha_1^* + \alpha_2^*) / 2 \quad (19)$$

Another controller that is shown in Fig.7. is battery controller where battery is incorporated within the PV system configuration in order to provide or absorb active power and support the frequency control objective with the PV generator. If there is superabundant solar energy and therefore the active power needed for frequency control is a smaller amount than PV MPP, then the battery are going to be charged. If there's not

enough solar energy obtainable and if the active power needed for frequency control is over PV MPP, then the battery can offer the deficit power so as to maintain the microgrid frequency at 60 Hz.

The PI controller,  $PI_5$  revises error signal after differencing the actual battery power  $P_{batt}$  with the battery reference value,  $P_{Battref}$ . This signal is compared with a triangular waveform magnitude to generate a signal,  $S^*$ . The equation for this control is given by (20)

$$S^* = K_{p5}(P_{Battref} - P_{Batt}) + K_{I5} \int_0^t (P_{Battref} - P_{Batt}) dt \tag{20}$$

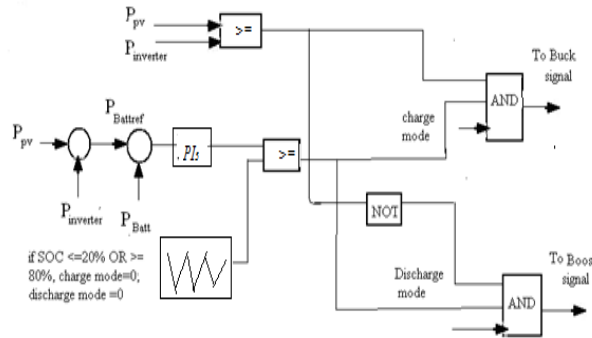


Fig. 7: Battery power control diagram

**SIMULATION RESULTS AND DISCUSSION**

The system configuration for V-F control of solar output power integrated to grid concise of different modes with respect to variation in voltage and frequency of the system. In first mode, load is directly connected to grid. In this mode central controller controls both active and reactive power of the system to maintain voltage and frequency at rated value around 0.985 pu as shown in fig 8(a) and frequency of 60 HZ as shown in fig 8 (b) respectively.

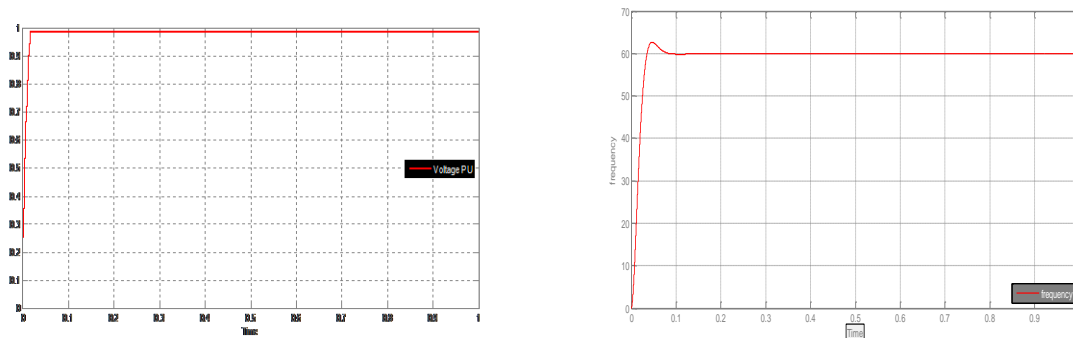


Fig.8: Results of coordinated V-f control when load connected to grid

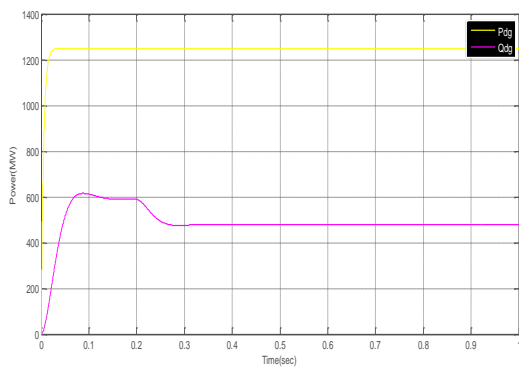
During second and third mode of the V-f control, irradiance of 1000 W/m<sup>2</sup> is considered. While moving from the grid connected to microgrid mode, the diesel generator is controlled to generate a fixed amount of 1.25 MW throughout the simulation period as shown in Fig. 9(a). It also shows the reactive power generated by the diesel generator is 0.5 MW. The PI controller gain parameters are given in Table 3. If irradiance changes, the controller gains ought to be adjusted slightly to minimize the error. By using IC controller to the solar PV and with respect to inverter PI controller. These controllers will calculate the error value of generation and load by that it send command to inverter controller which optimizes active and reactive power generation required to meet the load.

**Table 3:** Controller Gain Parameters

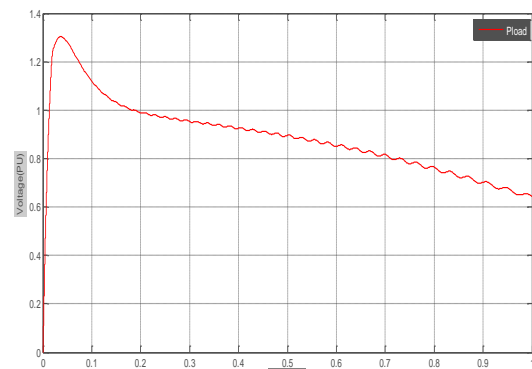
Type of Control Loop	Gain	Value
Voltage Control Loop	Kp2	0.0004
	Ki2	0.005
Frequency Control Loop	Kp3	9.9 X 10-4
	Ki3	5 X 10-3
Battery Control Loop	Kp5	1.5 X 10-8
	Ki5	1.5 X 10-7

In the islanded mode, the active power generated by the diesel generator isn't enough to fulfill the demand of the microgrid. Fig. 9(b) shows the plot of the PCC voltage is less than 0.6 p.u. Fig. 9(c) shows the microgrid frequency that fall to a value below 55Hz due to load-generation imbalance. Once the control is started, the solar PV generates 100kW active power but the active power, that is needed to take care of the frequency at 60 Hz is 80kW as shown in Fig. 9(d). The frequency control from the PV generator starts quickly and regulates the frequency back to 60 Hz as shown in Fig. 9(e). And Fig. 9 (f) shows the plot of the PCC voltage is 0.9 p.u. It is observed that voltage is also quickly regulated at around 1 p.u.

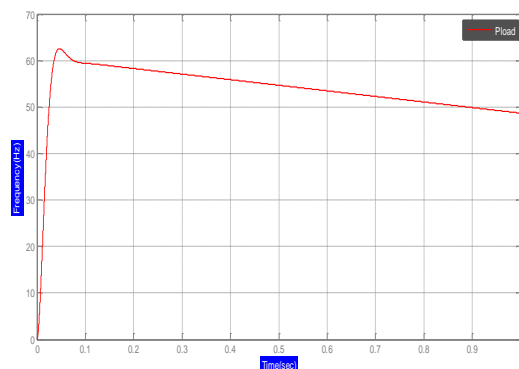
However, the load requires only 80 kW active power but the solar PV generates more than required that is evident from Fig. 9(d), which stores in energy storage batteries. For example considering solar irradiance is overabundant at 932W/m<sup>2</sup> and thus, the PV generates power of 85.9 kW. The excess 5.9 kW is employed to charge the battery. i.e., the battery absorbs power. For instance, if solar irradiance is less than the required, at particular irradiance PV generates solely around 75 kW. This is not sufficient to maintain the microgrid frequency at 60 Hz. Hence, the deficit power of around 5 kW is provided by the battery by using buck-boost controller. Battery state of charge (SOC) 80% is shown in fig. 9 (g).



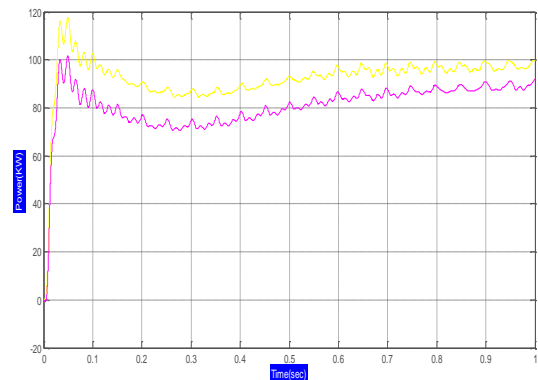
(a)



(b)



(c)



(d)



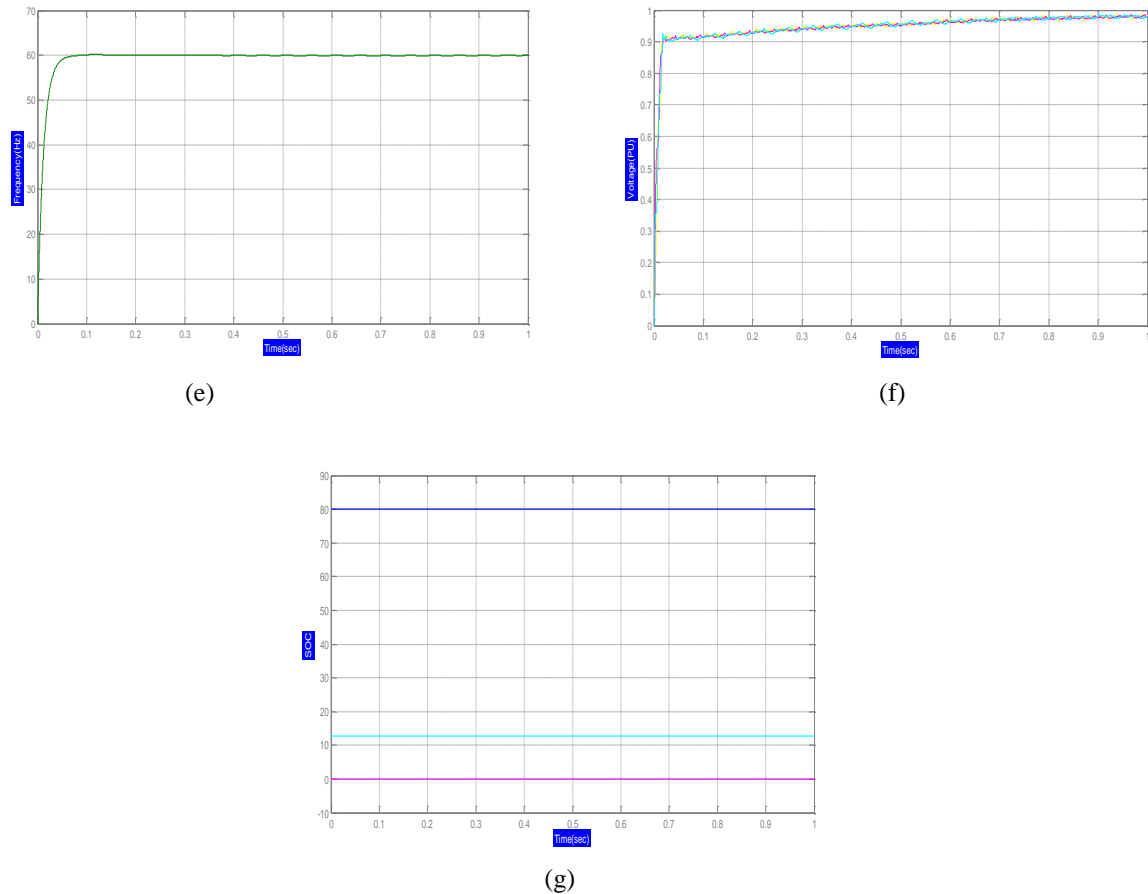


**Fig.9:** Results of coordinated V-f control when solar pv and diesel generator connected to load

## CONCLUSION

The control strategies of Incremental Conductance in MPPT of solar PV generators in islanded microgrid scenarios are proposed, investigated and valid. The response time of the PI control is incredibly short which implies that the controls will quickly track the load variation. This new simplified, effective MPPT and voltage control algorithmic rule is enforced for the peak utilization of the solar resource in providing the overall active power generation to the grid and at a similar time providing local voltage support. We have observed that if there change in the irradiation value there is change in the solar output power as we know irradiation is not constant thought out the day which effects voltage and frequency. So to improve this drawback battery storage is used with the help of buck-boost converter. The proposed V-f control technique shows satisfactory results with voltage and frequency back to the nominal value within a short time when compared to traditional strategies these methods offers terribly acceptable performance. In future control parameters are to be fine-tuned for considering the hourly variation in the irradiations levels.

## REFERENCES

- [ 1 ] Sarina Adhikari and Fangxing Li, Coordinated V-f and P-Q Control of Solar Photovoltaic Generators With MPPT and Battery Storage in Microgrids in Proc. IEEE Transactions On Smart Grid, vol. 5, no. 3, May 2014
- [ 2 ] R. H. Lasseter, "MicroGrids," in Proc. IEEE Power Engineering Society Winter Meeting, 2002, vol. 1, pp. 305–308
- [ 3 ] S. Chowdhury, S. P. Chowdhury, and P. Crossley, "Microgrids and Active Distribution Networks," 2009, IET Renewable Energy Series 6.
- [ 4 ] H. Saadat, Power System Analysis, 2nd ed. New York, NY, USA: Mc-Graw Hill, 2002.

- [ 5 ] J. A. P. Lopes, C. L. Moreira, and A. G. Madureira, "Defining control strategies for analysing microgrids islanded operation," in Proc. IEEE St. Petersburg PowerTech, St. Petersburg, Russia, 2005
- [ 6 ] B. Awad, J. Wu, and N. Jenkins, "Control of distributed generation," *Electrotechn. Info.* (2008), vol. 125/12, pp. 409–414.
- [ 7 ] J. M. Guerrero, J. Matas, L. Garcia de Vicuña, M. Castilla, and J. Miret, "Decentralized control for parallel operation of distributed generation inverters using resistive output impedance," *IEEE Trans. Ind. Electron.*, vol. 54, no. 2, April 2007, pp. 994–1004.
- [ 8 ] P. Arbolea, D. Diaz, J. Guerrero, P. Garcia, F. Briz, C. GonzalezMoran, and J. G. Alexandre, "An improved control scheme based in droopcharacteristicformicrogridconverters," *ElectricPowerSystems Research*, vol. 80, pp. 1215–1221, 2010.
- [ 9 ] T. L. Vandoorn, B. Renders, L. Degroote, B. Meersman, and L. Vandeveldel, "Active load control in islanded microgrids based on the grid voltage," *IEEE Trans. Smart Grid*, vol. 2, no. 1, pp. 139–151, Mar. 2011.
- [ 10 ] H. Laaksonen, P. Saari, and R. Komulainen, "Voltage and frequency control of inverter based weak LV network microgrid," presented at the Int. Conf. Future Power Syst., Amsterdam, The Netherlands, Nov.18, 2005.
- [ 11 ] J. C. Vasquez, R. A. Mastromauro, J. M. Guerrero and M. Liserre, "Voltage support provided by a droop-controlled multifunctional in- verter," *IEEE Trans. Ind. Electron.*, vol. 56, pp. 4510–4519, 2009.
- [ 12 ] D. N. Gaonkar, P. C. Rao, and R. N. Patel, "Hybrid method for voltage regulation of distribution system with maximum utilization of connected distributed generation source," in Proc. IEEE Power India Conf., 2006.
- [ 13 ] B. Kroposki, C. Pink, R. DeBlasio, H. Thomas, M. Simoes, and P.K.Sen, "Benefitsofpowerelectronicinterfacesfordistributedenergyresources," *IEEETrans.EnergyConvers.*, vol.25, no.3, pp.901–908, Sep. 2010.
- [ 14 ] L. D. Watson and J. W. Kimball, "Frequency regulation of a microgridusing solar power," in Proc. 2011 IEEE APEC, pp. 321–326
- [ 15 ] M. G. Molina and P. E. Mercado, "Modeling and control of grid-con- nected photovoltaic energy conversion system used as a dispersed gen- erator," in Proc. 2008 IEEE/PES Transm. Distrib. Conf. Expo.: LatinAmerica, pp. 1–8.
- [ 16 ] C.Luo,H.G.Far,H.Banakar,P.W.Keung,andB.T.Ooi, "Estimationofwindpenetrationaslimitedbyfrequencydeviation," *IEEETrans.Energy Convers.*, vol. 22, no. 3, pp. 783–791, Sep. 2007.
- [ 17 ] T. Ota, K. Mizuno, K. Yukita, H. Nakano, Y. Goto, and K.Ichiyanagi, "Study of load frequency control for a microgrid," in Proc. 2007AUPEC Power Eng. Conf., pp. 1–6.
- [ 18 ] H. Yang, W. Zhou, and L. Lu, "Optimal sizing method for stand-alone hybrid solar–wind system with LPSP technology by using genetic algorithm ," *Solar Energy*, vol. 82, pp.354–367, April 2008
- [ 19 ] D. Sera, R. Teodorescu, and P. Rodriguez, "PV panel model based on datasheet values," in Proc. IEEE Int. Symp. Ind. Electron. (ISIE), 2007, pp. 2392–2396.
- [ 20 ] Y. Xu, H. Li, D. T. Rzy, F. Li, and J. D. Kueck, "Instantaneous active and nonactive power control of distributed energy resources with a cur- rent limiter," in Proc. IEEE Energy Conversion Congr. Expo., 2010, pp. 3855–3861.